Journal of the Mechanics and Physics of Solids 59 (2011) 2259–2278

Contents lists available at SciVerse ScienceDirect

Journal of the Mechanics and Physics of Solids

journal homepage: www.elsevier.com/locate/jmps

Mechanics and chemical thermodynamics of phase transition in temperature-sensitive hydrogels

Shengqiang Cai, Zhigang Suo*

School of Engineering and Applied Sciences, Kavli Institute for Nanobio Science and Technology, Harvard University, Cambridge, MA 02138, USA

ARTICLE INFO

Article history:
Received 12 May 2011
Received in revised form
27 August 2011
Accepted 29 August 2011
Available online 1 September 2011

Keywords:
Elastomer
Phase transition
Temperature-sensitive hydrogel
Large deformation

ABSTRACT

This paper uses the thermodynamic data of aqueous solutions of uncrosslinked poly-(*N*-isopropylacrylamide) (PNIPAM) to study the phase transition of PNIPAM hydrogels. At a low temperature, uncrosslinked PNIPAM can be dissolved in water and form a homogenous liquid solution. When the temperature is increased, the solution separates into two liquid phases with different concentrations of the polymer. Covalently crosslinked PNIPAM, however, does not dissolve in water, but can imbibe water and form a hydrogel. When the temperature is changed, the hydrogel undergoes a phase transition: the amount of water in the hydrogel in equilibrium changes with temperature discontinuously. While the aqueous solution is a liquid and cannot sustain any nonhydrostatic stress in equilibrium, the hydrogel is a solid and can sustain nonhydrostatic stress in equilibrium. The nonhydrostatic stress can markedly affect various aspects of the phase transition in the hydrogel. We adopt the Flory–Rehner model, and show that the interaction parameter as a function of temperature and concentration obtained from the PNIPAM–water solution can be used to analyze diverse phenomena associated with the phase transition of the PNIPAM hydrogel. We analyze free swelling, uniaxially and biaxially constrained swelling of a hydrogel, swelling of a core–shell structure, and coexistent phases in a rod. The analysis is related to available experimental observations. Also outlined is a general theory of coexistent phases undergoing inhomogeneous deformation.

1. Introduction

A network of covalently crosslinked, long, and flexible polymer chains can aggregate with water to form an elastomeric hydrogel. When the hydrogel equilibrates with a surrounding aqueous solution, depending on the functional groups along the polymer chains, the amount of water in the hydrogel can be affected by many stimuli, including forces (Doi, 2009), temperature (Otake et al., 1990), pH (Marcombe et al., 2010), ionic concentration (Tanaka et al., 1980), and electric field (Shiga, 1997; Osada and Gong, 1998). The significance of mechanochemical interaction in hydrogels is vividly illustrated by the following example. In superabsorbent diapers, the granules of a hydrogel need to absorb water many times their own weight. The swollen diapers need to feel dry under the weights of babies (Masuda, 1994).

Stimuli-responsive hydrogels are being developed for diverse applications, such as microvalves (Richter et al., 2004), actuators (Carpi and Smela, 2009), and sensors (Lee and Braun, 2003). Many such applications require hydrogels to swell

* Corresponding author.
E-mail address: suo@seas.harvard.edu (Z. Suo).

0022-5096/$ - see front matter © 2011 Elsevier Ltd. All rights reserved.
doi:10.1016/j.jmps.2011.08.008

under the constraint of surrounding materials, or under external forces. For example, Steinberg et al. (1966) developed a mechanochemical engine, involving a collagen fiber swelling and shrinking in two baths of aqueous solutions of different ionic concentrations, while lifting a weight. As another example, Hu et al. (1995) used a temperature-sensitive hydrogel to fabricate a hand-like device, gripping or releasing objects by changing the temperature.

These and many other applications have motivated recent development of the nonlinear field theory of hydrogels (e.g., Baek and Srinivasa, 2004; Dolbow et al., 2004; Hui and Muralidharan, 2005; Li et al., 2007; Hong et al., 2008, 2009, 2010; Doi, 2009; Marcombe et al., 2010; Chester and Anand, 2010; An et al., 2010; Baek and Pence, 2011). The theory is formulated on the basis of the kinematics of network deformation, kinetics of water migration, and thermodynamics of swelling.

The field theory of hydrogels, however, involves multiple fields and nonlinear functions; quantitative comparison between theoretical predictions and experimental observations has been challenging. This paper takes advantage of a large number of available experiments of a particular polymer: poly(*N*-isopropylacrylamide) (PNIPAM). Specifically, we use the thermodynamic data of aqueous solutions of PNIPAM to analyze the behavior of PNIPAM hydrogels under various mechanical forces and constraints. At a low temperature, uncrosslinked PNIPAM can be dissolved in water and form a homogenous liquid solution (Fig. 1a). When the temperature is increased, the solution separates into two liquid phases with different concentrations of the polymer (Fig. 1b). Covalently crosslinked PNIPAM, however, does not dissolve in water, but can imbibe water and form a hydrogel. When the temperature is changed, the hydrogel undergoes a phase transition: the amount of water in the hydrogel in equilibrium changes with the temperature discontinuously (Fig. 2).

While the aqueous solution is a liquid and cannot sustain any nonhydrostatic stress in equilibrium, the hydrogel is a solid and can sustain nonhydrostatic stress in equilibrium. The nonhydrostatic stress can markedly affect various aspects of the phase transition in the hydrogel. Consequently, it is significant to show that the interaction parameter obtained from the solution can predict diverse phenomena associated with the phase transition of the hydrogel under nonhydrostatic stress.

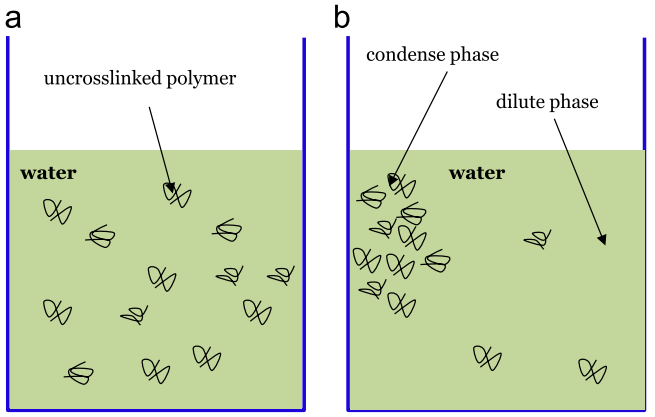

Fig. 1. Schematics of a temperature-sensitive polymer solution. (a) At a low temperature, the uncrosslinked polymers dissolve in water and form a homogenous solution. (b) At a high temperature, the solution separates into two liquid phases with different concentrations of the polymer.

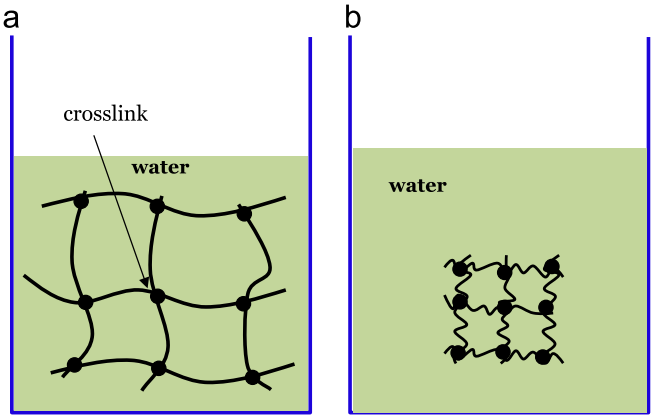

Fig. 2. Schematics of a temperature-sensitive hydrogel. (a) At a low temperature, the network absorbs a large amount of water, and the hydrogel is in the swollen phase. (b) At a high temperature, the network absorbs a small amount of water, and the hydrogel is in the shrunk phase.

The PNIPAM hydrogels have been studied extensively since 1950s, as a model system and for diverse applications; see the review by Schild (1992). For a hydrogel immersed in an aqueous environment and subject to mechanical forces, water molecules can migrate in and out the hydrogel. A recent study has compared the field theory and experiments concerning the kinetics of swelling (Yoon et al., 2010). To focus on the effect of mechanical constraints and forces on the phase transition, we will study the states of the hydrogel in equilibrium with the aqueous environment and mechanical forces, and will not study the time-dependent process of solvent migration. Associated with the phase transition, the volume of the hydrogel can change as large as 1000 times (Otake et al., 1990). Cho et al. (2003) and others have reviewed the molecular interactions underlying this phase transition. This paper will be concerned with macroscopic observations of how the phase transition is affected by mechanical constraints and forces.

For a piece of the hydrogel attached to a stiff substrate, the top part of the hydrogel, which is less constrained by the substrate, has a different phase-transition temperature from the bottom part of the hydrogel (Harmon et al., 2003). In a core–shell structure, the phase transition of a hydrogel core can be suppressed by a stiff elastomer shell (Berndt and Richtering, 2003). The phase-transition temperature can also be lowered by applying a pressure (Juodkazis et al., 2000). The phase transition of a rod of the hydrogel can be induced by applying a uniaxial force (Hirotsu and Onuki, 1989; Suzuki and Ishii, 1999). Various patterns of coexistent phases have been observed in hydrogels under constraints (Suzuki and Ishii, 1999; Bai and Suzuki, 1999).

Following previous works (e.g., Hong et al., 2008; Chester and Anand, 2010), this paper combines the thermodynamic theory of Gibbs and the Flory–Huggins statistical-mechanical model. The interaction between the polymers and water is described by a phenomenological parameter χ, which is a function of both the temperature and the volume fraction of the polymer. The interaction parameter χ has been fitted by Afroze et al. (2000) for the aqueous solutions of PNIPAM.

When the PNIPAM polymers are crosslinked by covalent bonds into a network, the crosslink density in the hydrogel is typically low, and each polymer chain consists of many monomers. We assume that the interaction parameter χ obtained from the PNIPAM-water solution can be used to study the phase transition of the PNIPAM hydrogel. Once the interaction parameter is fitted to the solution, the only additional fitting parameter for the hydrogel is the crosslink density.

Section 2 expresses stresses applied on a hydrogel in terms of a free-energy function and the chemical potential of water in the aqueous environment. Section 3 specifies the free-energy function according to the statistical mechanical model of Flory and Rehner (1943), accounting for the stretching of the network and the mixing of the network and the solution. The free energy of stretching is represented by the neo-Hookean model. The free energy of mixing is taken to be independent of the crosslinking of the polymers, and is fit to the available experimental data of aqueous solutions of uncrosslinked polymers (Afroze et al., 2000).

We then use the combined free energy of stretching and mixing to analyze crosslinked hydrogels. Section 4 considers free swelling hydrogels, uniaxially and biaxially constrained swelling hydrogels. Section 5 studies the phase transition of a core–shell structure. Section 6 studies coexistent phases in a rod of the hydrogel. We compare these analyses with experimental observations quantitatively when available experimental data are sufficiently complete, or qualitatively when trends of experimental observations have been reported. Section 7 outlines a general theory of coexistent phases undergoing inhomogeneous deformation.

2. A hydrogel in equilibrium with an aqueous environment and a set of forces

Fig. 3 illustrates a block of an elastomeric network. In the reference state, the block is a dry network, of dimensions L_1, L_2 and L_3. In the current state, the block is subject to forces P_1, P_2 and P_3, and is submerged in an aqueous environment of temperature T and of chemical potential of water μ. By convention, the chemical potential of water in pure liquid water

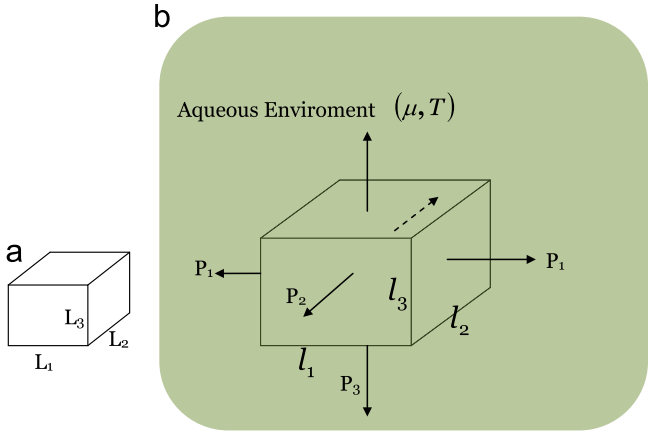

Fig. 3. (a) In the reference state, a dry network of polymers contains no water and is subject to no applied forces. (b) In the current state, the network is in equilibrium with applied forces, and with an aqueous environment of a fixed chemical potential of water and a fixed temperature.

is set to be zero. In the current state, the block absorbs M number of water molecules, and dimensions of the block become l_1, l_2 and l_3. Swelling is a highly entropic process. The Helmholtz free energy of the block in the current state is denoted as F.

When the block changes the dimensions by small amounts δl_1, δl_2 and δl_3, the applied forces do work $P_1\delta l_1+P_2\delta l_2+P_3\delta l_3$. When the number of water molecules in the block increases by δM, the chemical potential of water in the aqueous environment does work $\mu\delta M$. That is, the applied forces are work-conjugate to the displacements, and the chemical potential of water in the aqueous environment is work-conjugate to the number of water molecules. At a constant temperature, when the hydrogel equilibrates with the applied forces and the aqueous environment, the change in the Helmholtz free energy of the block equals the sum of the work done by the applied forces and the work done by the chemical potential of water

$$\delta F = P_1\delta l_1 + P_2\delta l_2 + P_3\delta l_3 + \mu\delta M. \tag{2.1}$$

This condition of equilibrium can also be interpreted in an alternative way. The gel, the forces and the aqueous environment together can be viewed as a composite system. The composite is held at a fixed temperature, and receives no work or matter from the rest of the world. The Helmholtz free energy of the composite is the sum of the Helmholtz free energy of the gel, the potential energy of the forces, and the Helmholtz free energy of the aqueous environment. That is, when P_1, P_2, P_3, μ are constant, the Helmholtz free energy of the composite is $F-P_1l_1-P_2l_2-P_3l_3-\mu M$. The parameters l_1, l_2, l_3 and M are internal variables of the composite system. The condition for the composite to equilibrate is that the variation of the Helmholtz free energy of the composite vanishes for arbitrary and independent variations of the internal variables.

In general, the dimensions of the block, l_1, l_2 and l_3, can vary independently from the number of water molecules in the hydrogel, M. The condition of equilibrium (2.1) holds for arbitrary and independent small variations of the four independent quantities: l_1, l_2, l_3 and M. In practice, however, the four quantities are connected by the following considerations (Hong et al., 2008). Upon imbibing water, the network swells. The two processes – imbibing and swelling – are connected. The volume of the block in the current state $l_1l_2l_3$, to a good approximation, equals the sum of the volume of the dry network $L_1L_2L_3$ and the volume of the absorbed water ΩM

$$l_1l_2l_3 = L_1L_2L_3 + \Omega M, \tag{2.2}$$

where Ω is the volume per water molecule. This approximation is commonly adopted in analyzing the swelling process of gels. (e.g., Flory and Rehner, 1943; Doi, 2009) The approximation generalizes the condition of incompressibility of elastomers, and is called molecular incompressibility (Hong et al., 2008).

The approximation of molecular incompressibility may be understood in terms of the following considerations. When water leaves a sponge, pores in the sponge remain open and are filled by air. In this regard, the sponge differs from a gel without macroscopic voids. In the gel, the polymer chains are long and flexible, interacting among themselves and with water molecules by weak intermolecular forces. When water molecules enter the gel, the polymer chains stretch and move apart to accommodate. When water molecules migrate out the gel, the polymer chains coil back and move together, leaving no voids behind. The forces applied to the hydrogel are typically small, and do not appreciably change the volumes of individual polymer chains or water molecules. When two species of molecules mix, the volume of the mixture usually differs from the sum of the volumes of the two pure components. This change in volume, however, is typically small compared to the change in volume during swelling (e.g., Eichinger and Flory, 1968; Eliassi et al., 1999; Sastry and Patel, 2003).

The relation (2.2) places a constraint among the four variables l_1, l_2, l_3 and M. We will regard l_1, l_2 and l_3 as independent variables, in term of which we express M using (2.2). Consequently, the variation of the number of water molecules in the hydrogel relates to the variations of the dimensions

$$\delta M = \frac{l_2l_3}{\Omega}\delta l_1 + \frac{l_1l_3}{\Omega}\delta l_2 + \frac{l_1l_2}{\Omega}\delta l_3. \tag{2.3}$$

Inserting (2.3) into (2.1), we obtain that

$$\delta F = \left(P_1 + \frac{l_2l_3\mu}{\Omega}\right)\delta l_1 + \left(P_2 + \frac{l_1l_3\mu}{\Omega}\right)\delta l_2 + \left(P_3 + \frac{l_1l_2\mu}{\Omega}\right)\delta l_3. \tag{2.4}$$

This condition of equilibrium holds for arbitrary and independent variations δl_1, δl_2 and δl_3.

For the time being, the deformation of the block is assumed to be homogeneous, but possibly anisotropic. Define the nominal concentration of water by $C=M/L_1L_2L_3$, and stretches by $\lambda_1=l_1/L_1$, $\lambda_2=l_2/L_2$ and $\lambda_3=l_3/L_3$. Dividing both sides of (2.2) by the volume of the dry elastomer, $L_1L_2L_3$, we obtain that

$$\lambda_1\lambda_2\lambda_3 = 1 + \Omega C. \tag{2.5}$$

This expression places a constraint among the four variables: λ_1, λ_2, λ_3 and C.

Define the nominal density of the Helmholtz free energy by $W=F/(L_1L_2L_3)$, true stresses by $\sigma_1=P_1/(l_2l_3)$, $\sigma_2=P_2/(l_1l_3)$ and $\sigma_3=P_3/(l_1l_2)$. Dividing both sides of Eq. (2.4) by $L_1L_2L_3$, we obtain that

$$\delta W = \left(\sigma_1 + \frac{\mu}{\Omega}\right)\lambda_2\lambda_3\delta\lambda_1 + \left(\sigma_2 + \frac{\mu}{\Omega}\right)\lambda_1\lambda_3\delta\lambda_2 + \left(\sigma_3 + \frac{\mu}{\Omega}\right)\lambda_1\lambda_2\delta\lambda_3. \tag{2.6}$$

This condition of equilibrium holds for arbitrary and independent variations $\delta\lambda_1$, $\delta\lambda_2$ and $\delta\lambda_3$.

As a material model, the nominal density of the free energy is taken to be a function of four independent variables

$$W = W(\lambda_1,\lambda_2,\lambda_3,T). \tag{2.7}$$

Due to the constraint (2.5), the concentration of water is excluded from the list of the independent variables in (2.7). At a fixed temperature, when the block deforms by small amounts, $\delta\lambda_1$, $\delta\lambda_2$ and $\delta\lambda_3$, the free energy varies by

$$\delta W = \frac{\partial W}{\partial \lambda_1}\delta\lambda_1 + \frac{\partial W}{\partial \lambda_2}\delta\lambda_2 + \frac{\partial W}{\partial \lambda_3}\delta\lambda_3. \tag{2.8}$$

A combination of (2.6) and (2.8) gives that

$$\left[\frac{\partial W}{\partial \lambda_1} - \left(\sigma_1 + \frac{\mu}{\Omega}\right)\lambda_2\lambda_3\right]\delta\lambda_1 + \left[\frac{\partial W}{\partial \lambda_2} - \left(\sigma_2 + \frac{\mu}{\Omega}\right)\lambda_1\lambda_3\right]\delta\lambda_2 + \left[\frac{\partial W}{\partial \lambda_3} - \left(\sigma_3 + \frac{\mu}{\Omega}\right)\lambda_1\lambda_2\right]\delta\lambda_3 = 0. \tag{2.9}$$

When the hydrogel equilibrates with the aqueous environment and the applied forces, (2.9) holds for arbitrary and independent variations $\delta\lambda_1$, $\delta\lambda_2$ and $\delta\lambda_3$. Consequently, the coefficient in front of each of the three variations in (2.9) must vanish, leading to three equations

$$\sigma_1 = \frac{\partial W(\lambda_1,\lambda_2,\lambda_3,T)}{\lambda_2\lambda_3\partial\lambda_1} - \frac{\mu}{\Omega}, \tag{2.10}$$

$$\sigma_2 = \frac{\partial W(\lambda_1,\lambda_2,\lambda_3,T)}{\lambda_1\lambda_3\partial\lambda_2} - \frac{\mu}{\Omega}, \tag{2.11}$$

$$\sigma_3 = \frac{\partial W(\lambda_1,\lambda_2,\lambda_3,T)}{\lambda_1\lambda_2\partial\lambda_3} - \frac{\mu}{\Omega}. \tag{2.12}$$

When the function $W(\lambda_1,\lambda_2,\lambda_3,T)$ is specified for a hydrogel, (2.10)–(2.12), along with (2.5), constitute the equations of state. For a given temperature T, the four equations of state relate eight variables: λ_1, λ_2, λ_3,C, σ_1, σ_2, σ_3, μ.

The equations of state describe the mechanochemical interaction of the hydrogels. In particular, the term μ/Ω has the dimension of stress, and is known as the pore pressure in poroelasticity, and as the water potential in plant physiology. The effect of μ/Ω is readily understood by considering a block of a hydrogel confined in a rigid and porous box. The box constrains the hydrogel to fixed dimensions, but permeable to water. When the chemical potential of water in the aqueous environment is increased, to keep the dimensions fixed, the hydrogel develops an additional pressure. This mechanochemical interaction is clearly indicated by (2.10)–(2.12).

3. The free energy function

The thermodynamic theory in the previous section leaves the free-energy function $W(\lambda_1,\lambda_2,\lambda_3,T)$ unspecified. This section specifies the free-energy function using an existing statistical mechanical model and experimental data. We now discuss a particular way to specify the nominal density of the Helmholtz free energy as a function of stretches $W(\lambda_1,\lambda_2,\lambda_3,T)$.

In many gels, the density of the crosslinks is very low. For example, each polymer chain may consist of over a thousand monomers. Consequently, to the first approximation, we may neglect the effect of the crosslinks on solution, and simply write the free energy of the gel as the sum

$$W = W_{mix} + W_{stretch}, \tag{3.1}$$

where W_{mix} is the free energy due to the mixing of the polymers and the solvent and $W_{stretch}$ is the free energy due to the stretching of the network.

In this paper, the Helmholtz free energy of mixing is taken to be of the form (Flory, 1942; Huggins, 1941)

$$W_{mix} = kT\left[C\log\frac{\Omega C}{1+\Omega C} + \frac{\chi C}{1+\Omega C}\right], \tag{3.2}$$

where kT is the temperature in the unit of energy, $\Omega = 3\times10^{-29}\,\mathrm{m}^3$ is the volume per water molecule, and χ a dimensionless measure of the strength of pairwise interactions between species. This parameter χ is used to fit experimental data in the following form (Huggins, 1964):

$$\chi(T,\phi) = \chi_0 + \chi_1\phi, \tag{3.3}$$

where

$$\chi_0 = A_0 + B_0T, \quad \chi_1 = A_1 + B_1T, \tag{3.4}$$

and

$$\phi = \frac{1}{1+\Omega C}, \tag{3.5}$$

is the volume fraction of the polymer in the hydrogel. We will be concerned with aqueous solutions and hydrogels of low concentrations of the polymer. Consequently, the parameter χ is taken to be a linear function of the concentration of the

polymer, (3.3). The free energy of mixing is assumed to be independent of the crosslink density. In particular, the free energy of mixing of a gel is taken to be the same as that of a solution.

For polymer chains crosslinked into a three-dimensional network, the stretching of the network causes a reduction in the entropy of the network. The Helmholtz free energy due to the stretching of the network is taken to be (Flory, 1953)

$$W_{stretch}=\frac{1}{2}NkT[\lambda_1^2+\lambda_2^2+\lambda_3^2-3-2\log(\lambda_1\lambda_2\lambda_3)], \tag{3.6}$$

where N is the nominal density of the polymer chains, namely, the number of polymer chains divided by the volume of the dry polymer.

Inserting the above free-energy function into (2.10)–(2.12), and using the constraint (2.5), we obtain that

$$\frac{\sigma_1\Omega}{kT}=\frac{N\Omega}{\lambda_1\lambda_2\lambda_3}(\lambda_1^2-1)+\log\left(1-\frac{1}{\lambda_1\lambda_2\lambda_3}\right)+\frac{1}{\lambda_1\lambda_2\lambda_3}+\left(\frac{\chi_0-\chi_1}{\lambda_1^2\lambda_2^2\lambda_3^2}+2\frac{\chi_1}{\lambda_1^3\lambda_2^3\lambda_3^3}\right)-\frac{\mu}{kT}, \tag{3.7}$$

$$\frac{\sigma_2\Omega}{kT}=\frac{N\Omega}{\lambda_1\lambda_2\lambda_3}(\lambda_2^2-1)+\log\left(1-\frac{1}{\lambda_1\lambda_2\lambda_3}\right)+\frac{1}{\lambda_1\lambda_2\lambda_3}+\left(\frac{\chi_0-\chi_1}{\lambda_1^2\lambda_2^2\lambda_3^2}+2\frac{\chi_1}{\lambda_1^3\lambda_2^3\lambda_3^3}\right)-\frac{\mu}{kT}, \tag{3.8}$$

$$\frac{\sigma_3\Omega}{kT}=\frac{N\Omega}{\lambda_1\lambda_2\lambda_3}(\lambda_3^2-1)+\log\left(1-\frac{1}{\lambda_1\lambda_2\lambda_3}\right)+\frac{1}{\lambda_1\lambda_2\lambda_3}+\left(\frac{\chi_0-\chi_1}{\lambda_1^2\lambda_2^2\lambda_3^2}+2\frac{\chi_1}{\lambda_1^3\lambda_2^3\lambda_3^3}\right)-\frac{\mu}{kT}, \tag{3.9}$$

Eqs. (3.7)–(3.9), along with (2.5), constitute the equations of state of temperature-sensitive hydrogels. Given the temperature T, the chemical potential of water μ, and the applied stresses σ_1, σ_2 and σ_3, (3.7)–(3.9) are a set of nonlinear equations that determine the three stretches λ_1, λ_2 and λ_3. Once the stretches are determined, (2.5) gives the concentration of water in the hydrogel. The equations of state has a single adjustable material parameter, $N\Omega$, which is a dimensionless measure of the crosslink density.

In all numerical examples in the following sections, the hydrogel is assumed to be submerged in pure liquid water. Consequently, when the hydrogel reaches a state of equilibrium, the chemical potential of water in the hydrogel attains the value $\mu=0$.

Afroze et al. (2000) studied the PNIPAM–water solutions at various temperatures and concentrations, and fitted their experimental data by using the following parameters:

$$A_0=-12.947,\ B_0=0.04496K^{-1},\ A_1=17.92,\ B_1=-0.0569K^{-1} \tag{3.10}$$

These parameters determined for the PNIPAM–water solutions will be used to predict the behavior of phase transition of PNIPAM hydrogels.

4. Several cases of homogenous deformation

As stated in the Section 1, we assume that the molecular interaction in the PNIPAM–water solution remains unchanged in the PNIPAM hydrogel. Consequently, once the interaction parameter is fitted to the solution, the only additional fitting parameter for the hydrogel is the crosslink density. To ascertain this assumption, the material model described above is now applied to several cases of homogenous deformation as illustrated in Fig. 4. The predictions of the model will be compared with available experimental data.

When a network is submerged in an aqueous environment and is subject to no mechanical constraint, the network imbibes water and swells freely (Fig. 4a). Such free swelling has long been characterized by measuring the volume of the hydrogel as a function of temperature (Schild, 1992; Suzuki et al., 1999; Oh et al. 1998). In equilibrium, the hydrogel swells by the same stretch in all directions, so that

$$\lambda_1=\lambda_2=\lambda_3=\left(\frac{V}{V_0}\right)^{1/3}, \tag{4.1}$$

where V is the volume of the hydrogel in the current state, and V_0 is the volume of the dry polymer. Using expressions in Section 3, we specialize the Helmholtz free energy of the free-swelling hydrogel as

$$W\left(\frac{V}{V_0},T\right)=\frac{1}{2}NkT\left[3\left(\frac{V}{V_0}\right)^{2/3}-3-2\log\left(\frac{V}{V_0}\right)\right]+\frac{kT}{\Omega}\left[\left(\frac{V}{V_0}-1\right)\log\left(1-\frac{V_0}{V}\right)+\chi\left(1-\frac{V_0}{V}\right)\right] \tag{4.2}$$

Fig. 5(a) plots the free energy (4.2) as a function of the volume at several temperatures. The crosslink density is set to be $N\Omega=0.01$. At a low temperature ($T=304$ K), the free-energy function W has a single minimum at a large volume, corresponding to a stable state of equilibrium, the swollen state. At a high temperature ($T=306$ K), the free-energy function has a single minimum at a small volume, corresponding to a stable state of equilibrium, the shrunk state. For an intermediate range of temperature, the free energy function has two local minima and one local maximum: the lower minimum corresponds to a stable state of equilibrium, the higher minimum corresponds to a metastable state of equilibrium, and the maximum corresponds to an unstable state of equilibrium.

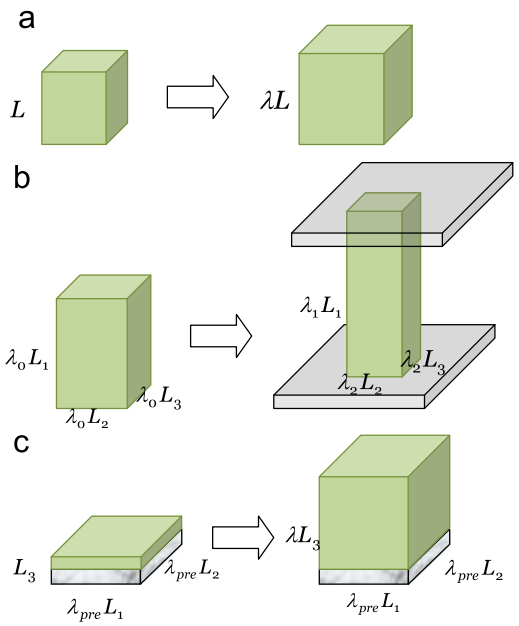

Fig. 4. Several cases of homogenous deformation. (a) Free swelling (b) swelling subject uniaxial constraint and (c) swelling subject to biaxial constraint.

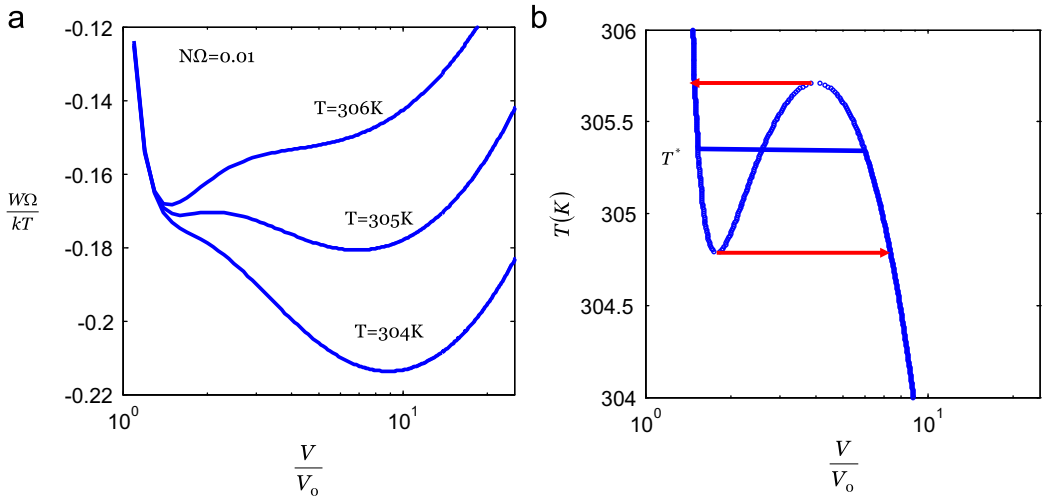

Fig. 5. A hydrogel is in equilibrium with water and is subject to no applied forces. (a) The Helmholtz free energy as a function of volume is plotted at several temperatures. At a high temperature, the free energy has a single minimum at a small volume, corresponding to the shrunk phase. At a low temperature, the free energy has a single minimum at a large volume, corresponding to the swollen phase. At an intermediate temperature, the free energy has two local minima and one local maximum. (b) The volume that minimizes and maximizes the free energy is plotted for the hydrogel at various temperatures. At a particular temperature T^*, the two minima of the free energy have the same value.

For the free energy W to reach a local minimum or maximum, the first-order derivative of W with respect to V/V_0 should vanish

$$\frac{\partial W(V/V_0,T)}{\partial(V/V_0)}=0 \tag{4.3}$$

Applying this condition to the free-energy function (4.2), we obtain that

$$N\Omega\left[\left(\frac{V}{V_0}\right)^{-1/3}-\left(\frac{V}{V_0}\right)^{-1}\right]+\log\left[1-\left(\frac{V}{V_0}\right)^{-1}\right]+\left(\frac{V}{V_0}\right)^{-1}+(\chi_0-\chi_1)\left(\frac{V}{V_0}\right)^{-2}+2\chi_1\left(\frac{V}{V_0}\right)^{-3}=0 \tag{4.4}$$

This condition of equilibrium can also be obtained from (3.7) by setting $\sigma_1=0$, $\mu=0$, and $\lambda_1=\lambda_2=\lambda_3=(V/V_0)^{1/3}$. Because χ_0 and χ_1 are linear in temperature, (4.4) defines temperature as a function of volume. This function is plotted in Fig. 5 (b). The shape of the curve is expected from the above description of the free-energy function.

At a particular temperature T^*, the free-energy function has two local minima at different volumes V' and V'', but the two minima have the same value of the free energy, namely

$$W\left(\left(\frac{V'}{V_0}\right),T^*\right)=W\left(\left(\frac{V''}{V_0}\right),T^*\right). \tag{4.5}$$

The position of T^* is identified in Fig. 5(b). If T^* is taken as the phase-transition temperature, associated with the phase transition, the volume of the hydrogel changes by

$$\Delta V=V''-V' \tag{4.6}$$

The experimentally observed volume–temperature curve upon heating often differs from that upon cooling (Linden et al., 2004; Guenther et al., 2007). Similar hysteresis is commonly observed for many types of phase transition. A possible hysteresis loop is indicated in Fig. 5 (b).

By searching for the global minimum of the free-energy function at every temperature, we can plot the volume–temperature curve (Fig. 6). Also plotted are the experimental data of Oh et al. (1998) for three different crosslink densities and the data of Suzuki et al. (1999). Since the crosslink densities of the PNIPAM gel in the experiments have not reported in the paper (Oh et al., 1998; Suzuki et al., 1999), $N\Omega$ is a fitting parameter for the comparisons in Fig. 6. A change in the crosslink density slightly changes the phase-transition temperature, but significantly changes the volume of the swollen phase. These theoretical predictions agree with experimental observations (Shibayama et al., 1997; Oh et al., 1998).

Fig. 4b illustrates a hydrogel bar with fixed stretch in the longitudinal direction. The hydrogel is assumed to be in a homogeneous but anisotropic state of swelling. According to the experiments carried out by Suzuki et al. (1997), the gel bar is first submerged in water at 303 K and reaches equilibrium with a homogenous and isotropic swelling ratio λ_0, and subsequently, the gel bar is stretched in the longitudinal direction with fixed length. Write the stretch in the longitudinal direction by λ_1. The hydrogel, however, is free to swell in the lateral direction and denote the stretch by λ_2. The volumetric swelling ratio relates to the stretches in the three directions as

$$\frac{V}{V_0}=(\lambda_2)^2\lambda_1. \tag{4.7}$$

Using (4.7), we write the free energy of the substrate-attached hydrogel as

$$W\left(\frac{V}{V_0},T\right)=\frac{NkT}{2}\left[2\left(\frac{V}{\lambda_1 V_0}\right)+\lambda_1^2-1-2\log\left(\frac{V}{V_0}\right)\right]+\frac{kT}{\Omega}\left[\left(\frac{V}{V_0}-1\right)\log\left(1-\frac{V_0}{V}\right)+\chi\left(1-\frac{V_0}{V}\right)\right]. \tag{4.8}$$

By searching for the global minimum of the free-energy function, we plot the volume–temperature curves in Fig. 7 for three levels of longitudinal stretch. Also plotted are the experimental data of Suzuki et al. (1997). The three curves predicted by the model reach a reasonable agreement with the theoretical predictions with only one adjustable parameter $N\Omega=0.01$.

Fig. 4c illustrates a thin layer of gel attached to a rigid substrate. The thickness of the layer is much smaller than the dimensions in the plane of the layer, and the hydrogel is assumed to be in a homogeneous but anisotropic state of swelling. When the hydrogel is submerged in water, the stretches in the two directions in the plane of the layer cannot change from

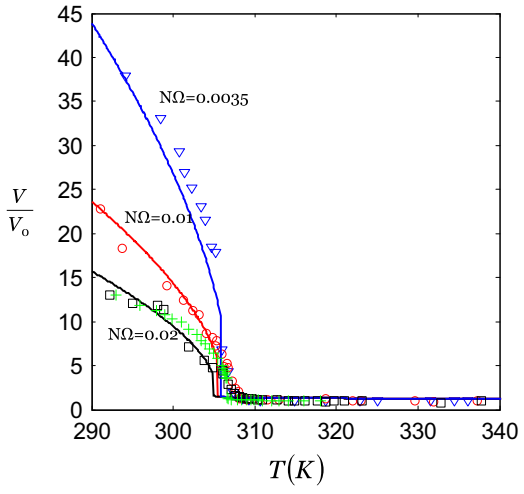

Fig. 6. The volumes of free-swelling hydrogels as functions of temperature. The solid curves are calculated for hydrogels of three values of the crosslink density. The triangle, circle and square symbols are experimental data for different crosslink density taken from Oh et al. (1998) and the cross symbols are experimental data taken from Suzuki et al. (1999).

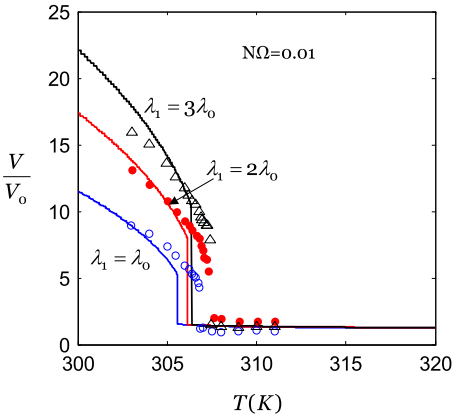

Fig. 7. The volumes of uniaxially constrained-swelling hydrogels as functions of temperature. The solid curves are calculated for hydrogels of three levels of longitudinal stretches. The triangle, circle and square symbols are experimental data for the corresponding longitudinal stretches taken from Suzuki et al. (1997).

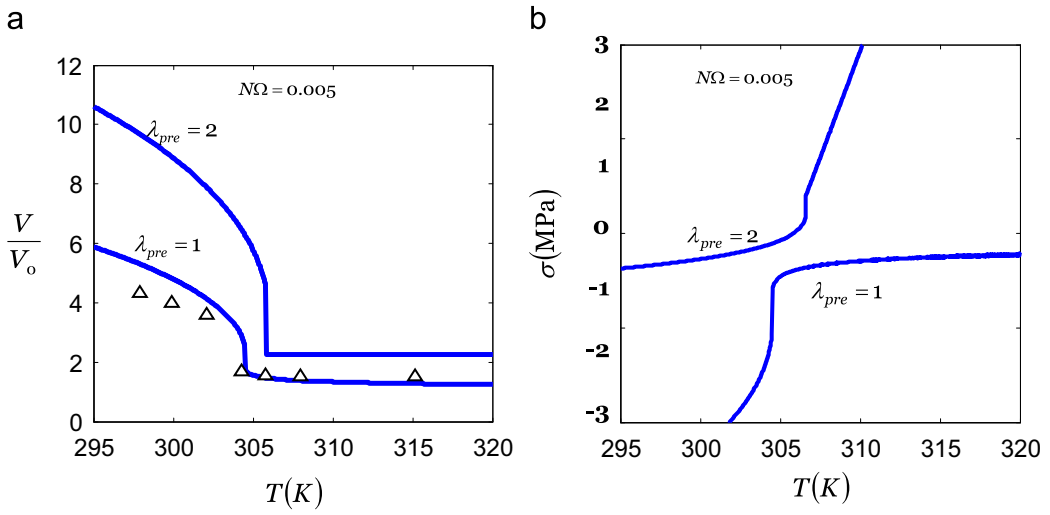

Fig. 8. A hydrogel with pre-swelling ratio λ_{pre} is bonded to a rigid substrate, and then subsequently swells in the direction normal to the substrate (inset). (a) The volumes as functions of temperature. The solid curves are calculated for hydrogels with different amounts of pre-swelling, and the triangular symbols are experimental data taken from Vidyasagar et al. (2008). (b) Confining stresses for hydrogels of different amounts of pre-swelling as functions of temperature.

the pre-stretch λ_{pre} set by the fabrication process, namely

$$\lambda_1 = \lambda_2 = \lambda_{pre}. \tag{4.9}$$

The hydrogel, however, is free to swell in the direction normal to the plane. Denote the stretch normal to the plane by $\lambda = \lambda_3$. The volumetric swelling ratio relates to the stretches in the three directions as

$$\frac{V}{V_0} = (\lambda_{pre})^2 \lambda. \tag{4.10}$$

Using (4.9) and (4.10), we write the free energy of the substrate-attached hydrogel as

$$W\left(\frac{V}{V_0}, T\right) = \frac{NkT}{2}\left[\left(\frac{V}{\lambda_{pre}^2 V_0}\right)^2 + 2\lambda_{pre}^2 - 1 - 2\log\left(\frac{V}{V_0}\right)\right] + \frac{kT}{\Omega}\left[\left(\frac{V}{V_0} - 1\right)\log\left(1 - \frac{V_0}{V}\right) + \chi\left(1 - \frac{V_0}{V}\right)\right] \tag{4.11}$$

By searching for the global minimum of the free-energy function, we plot the volume–temperature curves in Fig. 8(a). Also plotted are the experimental data of Vidyasagar et al. (2008), which reach a reasonable agreement with the theoretical predictions when we set $\lambda_{pre} = 1$ and $N\Omega = 0.005$.

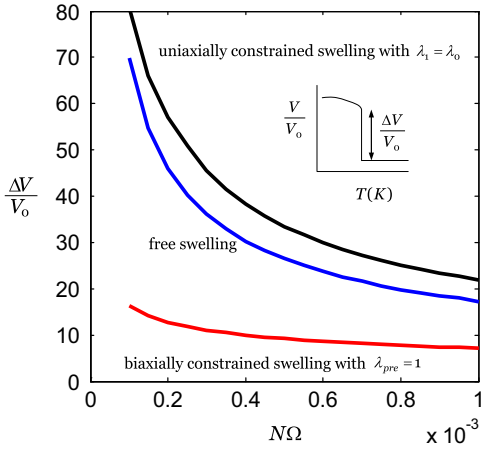

Fig. 9. Changes in the volume associated with the phase transition as a function of crosslink density.

The constrained hydrogel develops equal-biaxial stresses, $\sigma_1 = \sigma_2$. The magnitude of the stresses can be determined by inserting the stretches described above into (3.7). Fig. 8(b) plots the stress–temperature curves for two values of the pre-stretch. The magnitude of the stress changes discontinuously when the hydrogel undergoes the phase transition. Depending on the value of the pre-stretch and the temperature, the stress can be either tensile or compressive.

Actuators and sensors are often fabricated by attaching a layer of a hydrogel on the top of a layer of an elastic material (Hu et al., 1995; Bashir et al., 2002). The bilayer structure can be bent by the swelling-induced stress. Consequently, the stress in the hydrogel can be determined by measuring the radius of curvature (Yoon et al., 2010). At this writing, we are unable to find a complete set of experimental data to compare with our theoretical predictions.

Although the mechanical constraint has little influence on the phase-transition temperature, as shown in Figs. 6–8, the mechanical constraint can markedly affect the change in the volume of the hydrogel associated with the phase transition, Fig. 9. The change in the volume is reduced for a hydrogel of a high crosslink density.

5. Swelling of a core–shell structure

The effect of mechanical constraint on the phase transition has also been demonstrated experimentally by using a core–shell structure (Berndt et al., 2006a). This phenomenon is analyzed here. Fig. 10 sketches a spherical core–shell structure submerged in water. The core is a PNIPAM hydrogel, and the shell is an elastomer. The elastomer is incompressible, but is permeable to water. The structure is so prepared that, in equilibrium with the surrounding water, both the core and the shell are stress-free at a low temperature T_f; the hydrogel core is of radius A, and the elastomer shell is of outer radius B. In this stress-free state, the core is swollen and the stretch λ_f relates to T_f through the stretch–temperature curve of the hydrogel under the free-swelling condition. At a high temperature T, in equilibrium with the surrounding water, the hydrogel core exudes water and shrinks; the structure is in a stressed state: the core is of radius a, and the shell is of outer radius b.

In the stressed state at the temperature T, Fig. 10(b), the core is assumed to be bonded to the shell. The deformation of the core is homogenous and isotropic, with the stretches

$$\lambda_1 = \lambda_2 = \lambda_3 = \lambda_f \frac{a}{A}. \tag{5.1}$$

From Section 3, we obtain the nominal density of the free energy of the core

$$W_{core} = \frac{NkT}{2}\left[3\left(\frac{\lambda_f a}{A}\right)^2 - 3 - 6\log\left(\frac{\lambda_f a}{A}\right)\right] + \frac{kT}{\Omega}\left[\left(\frac{\lambda_f^3 a^3}{A^3} - 1\right)\log\left(1 - \frac{A^3}{\lambda_f^3 a^3}\right) + \chi\left(1 - \frac{A^3}{\lambda_f^3 a^3}\right)\right] \tag{5.2}$$

This nominal density times the volume of the dry network gives the free energy of the core

$$F_{core} = \frac{4\pi}{3}\left(\frac{A}{\lambda_f}\right)^3 W_{core}. \tag{5.3}$$

Once deformed, the shell is in an anisotropic and inhomogeneous state. As illustrated in Fig. 10, an element of the elastomer is at distance R from the center of the core when the elastomer is undeformed, and the element moves to a place at distance r from the center of the core when the elastomer is deformed. The function $r(R)$ specifies the kinematics of the deformation of the entire shell. The elastomer is taken to be incompressible, so that the volume of any part of the shell

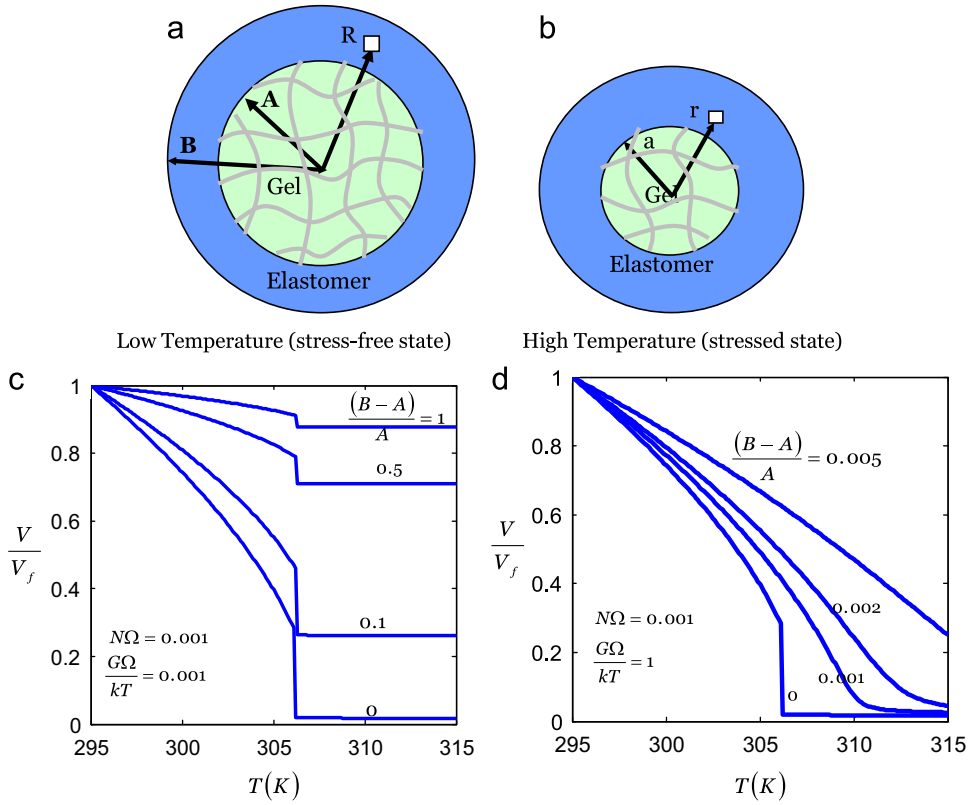

Fig. 10. A spherical core of a temperature-sensitive hydrogel is inside a shell of an elastomer. The elastomer allows water to permeate through, but swells negligibly. (a) At a low temperature, the core is swollen, and both the core and the shell are stress-free. (b) At a high temperature, the core contracts, and the shell is under compressive hoop stress. (c) The volume of the core–shell structure as a function of temperature, for a shell of a low modulus. (d) The volume of the core–shell structure as a function of temperature, for a shell of a high modulus.

remains unchanged during deformation, namely

$$r^3-a^3=R^3-A^3. \tag{5.4}$$

Consequently, the kinematics of the structure is fully determined once the radius of the core a is known—that is, the core–shell structure is a system of one degree of freedom. In particular, when the shell deforms, the volume of the shell remains unchanged

$$b^3-a^3=B^3-A^3. \tag{5.5}$$

This relation expresses the outer radius b in terms of the radius of the core a. The two hoop stretches are equal, given by

$$\lambda=r/R. \tag{5.6}$$

Due to incompressibility, the radial stretch is given by λ^{-2}. The elastomer is taken to be a neo-Hookean material, with the density of free energy

$$W_{shell}=\frac{G}{2}(2\lambda^2+\lambda^{-1}-3), \tag{5.7}$$

where G is the shear modulus of the elastomer. The free energy of the shell is $F_{shell}=\int W_{shell}dV$, where the integral extends over the volume of the elastomer. Using (5.4) and (5.6), we relate R to λ:$R^3=(a^3-A^3)/(\lambda^3-1)$. The element of volume can be written as $dV=(4\pi/3)d(R^3)=-4\pi(a^3-A^3)\lambda^2(\lambda^3-1)^{-2}d\lambda$. Consequently, the free energy of the shell is

$$F_{shell}=4\pi(a^3-A^3)\int_{b/B}^{a/A}\frac{W_{shell}(\lambda)\lambda^2 d\lambda}{(\lambda^3-1)^2}. \tag{5.8}$$

This integral is calculated numerically.

The total free energy of the structure, F, is the sum of the free energy of the core and that of the shell, namely

$$F=F_{core}+F_{shell}. \tag{5.9}$$

As mentioned above, the core–shell structure is a system of a single degree of freedom. Consequently, the free energy is a function of a single variable, $F(a)$. The state of equilibrium of the core–shell structure is determined by the radius of the core a that minimizes the free-energy function $F(a)$. This minimization can be carried out numerically.

The ratio of the volumes of the core–shell structure in the two states is $V/V_f=(b/B)^3$. Fig. 10(c) plots this ratio as a function of temperature. The calculation assumes that the stress-free state occurs at temperature $T_f=295$ K, crosslink density of the hydrogel is $N\Omega=0.001$, and the shear modulus of the elastomer is $G\Omega/kT=0.001$. The thickness of the shell affects the volume–temperature curves significantly, but only affects the phase-transition temperature slightly. These results qualitatively agree with experimental observations (Berndt et al., 2006b).

Fig. 10(d) plots the volume–temperature curves of the core–shell structure for the same core, but with a much stiffer shell, $G\Omega/kT=1$. Even with a very thin shell, the volume of the structure can vary smoothly with temperature, indicating that the stiff confinement suppresses the phase transition. A similar trend was reported by Berndt and Richtering (2003).

6. Coexistent phases in a rod of a hydrogel

Coexistent phases in a rod of an elastic material have long been studied (e.g., Ericksen, 1975; Abeyaratne and Knowles, 1988, 1993). Here we analyze the coexistent phases in a rod of a PNIPAM hydrogel, a phenomenon that has been demonstrated experimentally (Suzuki and Ishii, 1999).

The reference state is taken to be a rod of a dry network, length L and cross-sectional area A. We first consider a state of homogeneous deformation. When the rod is attached to a weight P, held at temperature T, and submerged in pure water ($\mu=0$), the length of the rod becomes l, and the cross-sectional area of the rod becomes a. The longitudinal stretch is $\lambda_3=l/L$, and the two transverse stretches are taken to be equal, $\lambda_1=\lambda_2=(a/A)^{1/2}$. The free energy function $W(\lambda_1,\lambda_3,T)$ can be specialized from Section 3.

The rod and the weight together constitute a thermodynamic system. The free energy of the system Π is the sum of the free energy of the hydrogel and the potential energy of the weight: $\Pi=WAL-Pl$. Consequently, the free energy of the system divided by the volume of the dry network is

$$G=W(\lambda_1,\lambda_3,T)-s\lambda_3, \tag{6.1}$$

where $s=P/A$ is the nominal stress. For a rod subject to a fixed temperature T and a fixed nominal stress s, thermodynamics requires that the equilibrium values of the stretches λ_1 and λ_3 should minimize the function $G(\lambda_1,\lambda_3)$.

Following Gibbs (1873), we first represent the condition of thermodynamic equilibrium graphically. Consider a three-dimensional space with (λ_1,λ_3) as the horizontal plane, and W as the vertical axis, Fig. 11. In this space, the function $W(\lambda_1,\lambda_3,T)$ at a given temperature is represented by a curved surface. The term $s\lambda_3$ is represented by an inclined plane passing through the λ_1 axis, with s as the slope of the inclined plane with respect to the λ_3 axis. By definition (6.1), G is the vertical distance between the curved surface and the inclined plane. Picture a plane simultaneously parallel to the inclined plane and tangent to the curved surface. Denote the tangent point by (λ_1,λ_3). Evident from the geometry, G is a local minimum if the curved surface in the neighborhood of the state (λ_1,λ_3) is above the tangent plane—that is, the curved surface is convex at the state (λ_1,λ_3).

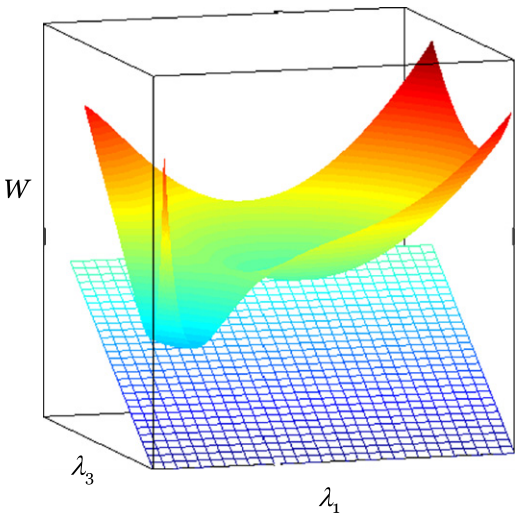

Fig. 11. The schematics of the Helmholtz free energy of a hydrogel deforming under the condition of equal transverse stretches $\lambda_1=\lambda_2$. The hydrogel is subject to no transverse stress, but is subject to an axial stress. The potential energy of the applied stress is represented by a plane passing the axis $\lambda_3=0$, with the slope of the plane being the axial stress. The vertical distance between the surface of the Helmholtz free energy and the loading plane is the Gibbs free energy. The Gibbs free energy is minimized by imagining a plane parallel to the loading plane and tangent to the surface of the Helmholtz free energy.

The above graphic representation can be expressed analytically. Imagine that the system is in a state (λ_1,λ_3), and is perturbed slightly to a state, $(\lambda_1+\delta\lambda_1,\lambda_3+\delta\lambda_3)$. The perturbation changes the free energy of the system by

$$\delta G=\frac{\partial W}{\partial\lambda_1}\delta\lambda_1+\left(\frac{\partial W}{\partial\lambda_3}-s\right)\delta\lambda_3+\frac{\partial^2 W}{2\partial\lambda_1^2}(\delta\lambda_1)^2+\frac{\partial^2 W}{2\partial\lambda_3^2}(\delta\lambda_3)^2+\frac{\partial^2 W}{\partial\lambda_1\partial\lambda_3}(\delta\lambda_1)(\delta\lambda_3). \tag{6.2}$$

This equation is the Taylor expansion of the function $G(\lambda_1,\lambda_3)$ up to the second order in $\delta\lambda_1$ and $\delta\lambda_3$. For G to reach a local minimum, the first-order variation must vanish

$$\frac{\partial W(\lambda_1,\lambda_3,T)}{\partial\lambda_1}=0, \tag{6.3}$$

$$\frac{\partial W(\lambda_1,\lambda_3,T)}{\partial\lambda_3}=s. \tag{6.4}$$

These two equations are similar to the equations of state (3.7) and (3.9), which we write in the following form:

$$N\Omega(\lambda_1^2-1)+\left(\frac{V}{V_0}\right)\log\left[1-\left(\frac{V}{V_0}\right)^{-1}\right]+1+(\chi_0-\chi_1)\left(\frac{V}{V_0}\right)^{-1}+2\chi_1\left(\frac{V}{V_0}\right)^{-2}=0, \tag{6.5}$$

$$\frac{1}{\lambda_3}\left[N\Omega(\lambda_3^2-1)+\left(\frac{V}{V_0}\right)\log\left[1-\left(\frac{V}{V_0}\right)^{-1}\right]+1+(\chi_0-\chi_1)\left(\frac{V}{V_0}\right)^{-1}+2\chi_1\left(\frac{V}{V_0}\right)^{-2}\right]=\frac{s\Omega}{kT}, \tag{6.6}$$

where $V/V_0=\lambda_1\lambda_2\lambda_3$ is the swelling ratio.

For the function $G(\lambda_1,\lambda_3)$ reaches a local minimum, the second-order variation in (6.2) must be positive-definite for arbitrary perturbations $\delta\lambda_1$ and $\delta\lambda_2$. This condition is equivalent to requiring that the Hessian

$$\mathbf{H}=\begin{bmatrix}\frac{\partial^2 W}{\partial\lambda_1^2} & \frac{\partial^2 W}{\partial\lambda_1\partial\lambda_3}\\ \frac{\partial^2 W}{\partial\lambda_1\partial\lambda_3} & \frac{\partial^2 W}{\partial\lambda_3^2}\end{bmatrix}, \tag{6.7}$$

should be positive-definite. For given values of T and s, to find a metastable state (i.e., a state that locally minimizes the function $G(\lambda_1,\lambda_3)$), we solve the algebraic equations (6.3) and (6.4) for λ_1 and λ_3, and then verify if the Hessian (6.7) is positive definite.

As the stress and the temperature vary, a local minimum may become a saddle point. That is, the Hessian may make a transition from a positive-definite matrix to an indefinite matrix. This transition occurs when

$$\det\mathbf{H}=0 \tag{6.8}$$

To illustrate these considerations, we imagine the following experiment. The temperature T is held fixed, while the stress s is changed gradually, allowing the hydrogel to equilibrate with the surrounding water. With reference to Fig. 11, the curved surface $W(\lambda_1,\lambda_3,T)$ is fixed. As the stress is changed gradually, the inclined plane rotates, and the tangent plane rolls along the curved surface. A sequence of tangent points forms a curve in the space, representing a sequence of states of equilibrium.

Fig. 12 plots this sequence of states of equilibrium on the (λ_1,λ_3), (λ_3,s), (λ_1,s) and $(V/V_0,s)$ planes for a hydrogel of a crosslink density $N\Omega=0.01$ and held at temperature $T=305.5$ K. A convenient way to plot these curves is to regard the swelling ratio V/V_0 as the independent variable, use (6.5) to express λ_1 in terms of V/V_0, write $\lambda_3=\lambda_1^{-2}V/V_0$, and then use (6.6) to express s in terms of V/V_0. The curves in Fig. 12 contain states that are either a minimum or a saddle point of the function $G(\lambda_1,\lambda_3)$ for given values of T and s. The shapes of the curves reflect that the surface $W(\lambda_1,\lambda_3,T)$ is non-convex.

For such a non-convex $W(\lambda_1,\lambda_3,T)$ showed in Fig. 11, as the tangent plane rolls, it may touch the curved surface at two points simultaneously at a particular value of the stress, s^*. Consequently, associated with the same stress s^*, two states of equilibrium exist, which we label as (λ_1',λ_3') and $(\lambda_1'',\lambda_3'')$. Marked in Fig. 12(b) are four states: A, B, C, and D. State A corresponds to the stress-free state. As the stress is increased to s^*, the hydrogel reaches state B. Then, without changing the stress, the hydrogel undergoes the phase transition from state B to state C, and the axial stretch jumps from λ'_3 to λ''_3. As the stress is increased further, the hydrogel deforms to state D. Recall that a free-swelling hydrogel undergoes the phase transition at temperature $T^*\approx 305.4$ K, Fig. 5. When the hydrogel is held at $T=305.5$ K, as in the present example, the hydrogel is in the shrunk phase. The hydrogel transforms to the swollen phase when a tensile stress $s*\approx 1$ MPa is applied, Fig. 12(b). That is, the phase-transition temperature is slightly affected by the uniaxial stress.

The four states A, B, C and D are also marked on the other three planes in Fig. 12. For example, Fig. 12(c) shows an interesting effect. In going from state A to state B, and from state C to state D, the hydrogel contracts in the transverse directions. In going from state B and C, however, the hydrogel expands in the transverse directions. This expansion is associated with the phase transition, during which the hydrogel swells by absorbing water. Consequently, under a tensile stress in the axial direction, form state A to state D, the hydrogel expands substantially in the transverse directions. This effect is reminiscent of a material with a negative Poisson's ratio.

The condition for the coexistent states can also be expressed analytically. Suppose that the rod is no longer homogenous, but is composed of segments of the two phases (Fig. 13). The transitional region in the rod between the

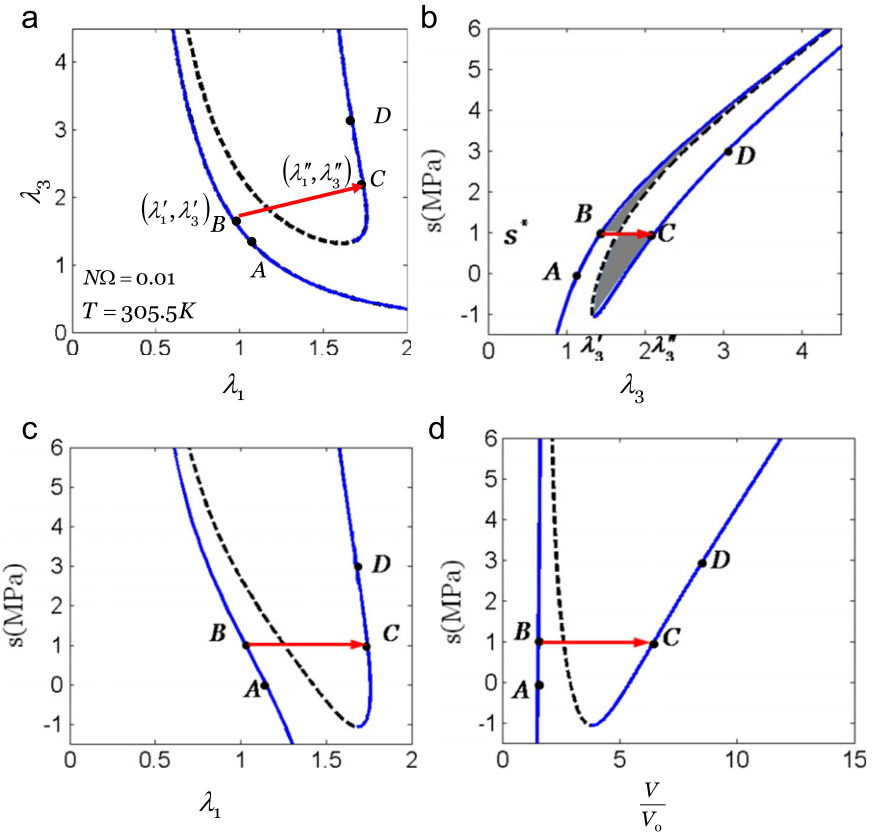

Fig. 12. A rod of a hydrogel is submerged in water, held at a constant temperature, and subject to an axial stress. As the axial stress increases, the hydrogel changes through a sequence of states of equilibrium. This sequence of states is represented as curves on various planes. The solid curves represent states corresponding to local minima of the free energy, the dashed curves represent states corresponding to saddle points of the free energy, and the arrows indicate the phase transition.

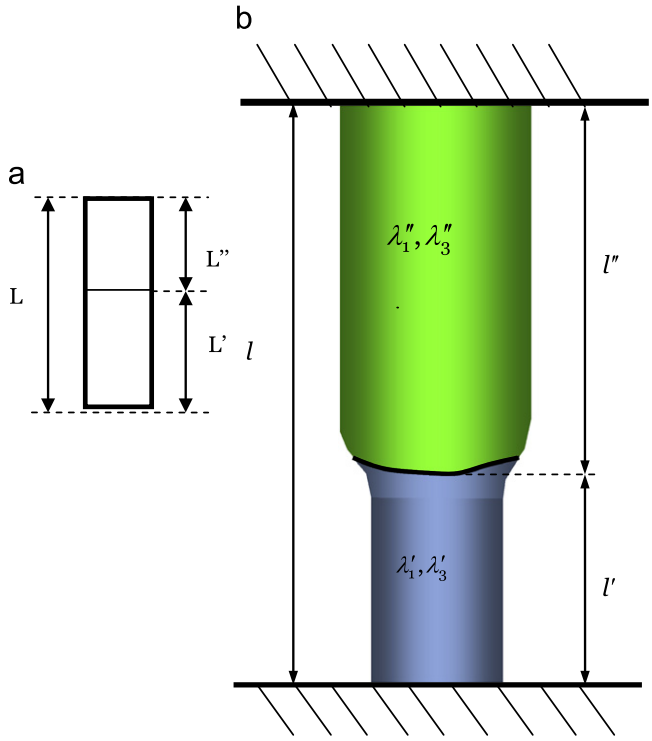

Fig. 13. In a rod of a hydrogel submerged in water, two phases of the hydrogel coexist in a state of equilibrium. (a) Reference and (b) current.

two phases is taken to be much shorter than the lengths of the two phases, and we will neglect the transitional region in this analysis. In the reference state, the two phases are of lengths L' and L'', and the total length of the rod is

$$L'+L''=L. \tag{6.9}$$

In the current state, the total length of the rod is

$$L'\lambda_3'+L''\lambda_3'=l. \tag{6.10}$$

When the rod is subject to an axial force P provided by a weight, the free energy of the composite system of the rod and the weight is

$$\Pi = AL'W(\lambda_1',\lambda_3',T)+AL''W(\lambda_1'',\lambda_3'',T)-sA(L'\lambda_3'+L''\lambda_3'). \tag{6.11}$$

This free energy is a function of five independent variables: $\Pi(\lambda_1',\lambda_3',\lambda_1'',\lambda_3'',L')$. Associated with the variations of the five variables, the free energy varies by

$$\begin{aligned}\delta\Pi = {} & AL'\frac{\partial W(\lambda_1',\lambda_3',T)}{\partial\lambda_1'}\delta\lambda_1'+AL''\frac{W(\lambda_1'',\lambda_3'',T)}{\partial\lambda_1''}\delta\lambda_1''+AL'\left[\frac{\partial W(\lambda_1',\lambda_3',T)}{\partial\lambda_3'}-s\right]\delta\lambda_3'+AL''\left[\frac{W(\lambda_1'',\lambda_3'',T)}{\partial\lambda_3''}-s\right]\delta\lambda_3''\\ & +A\left[W(\lambda_1',\lambda_3',T)-W(\lambda_1'',\lambda_3'',T)-s(\lambda_3'-\lambda_3'')\right]\delta L'\end{aligned} \tag{6.12}$$

Thermodynamics requires that in equilibrium the free energy be minimized. Because the five variables can vary independently, the coefficient in front each of the five variations mush vanish, giving that

$$\frac{\partial W(\lambda_1',\lambda_3',T)}{\partial\lambda_1'}=\frac{\partial W(\lambda_1'',\lambda_3'',T)}{\partial\lambda_1''}=0, \tag{6.13}$$

$$\frac{\partial W(\lambda_1',\lambda_3',T)}{\partial\lambda_3'}=\frac{\partial W(\lambda_1'',\lambda_3'',T)}{\partial\lambda_3''}=s, \tag{6.14}$$

$$W(\lambda_1'',\lambda_3'',T)-W(\lambda_1',\lambda_3',T)=s(\lambda_3''-\lambda_3') \tag{6.15}$$

Eqs. (6.13)–(6.15) are the conditions for the two phases to equilibrate with each other in the rod. Eq. (6.13) means that the transverse stresses in the two phases vanish, and (6.14) means that the axial stresses in the two phases equal the applied stress. Eq. (6.15) requires that the Gibbs free energies of the two phases should equal. These conditions are consistent with the geometrical interpretation discussed above: the two phases coexist in equilibrium when they lie on the common tangent plane of $W(\lambda_1,\lambda_3,T)$. The slope of the common tangent plane gives $s=s^*$, the particular value of the stress under which the two phases coexist in equilibrium.

Eq. (6.15) has a familiar graphic interpretation as Maxwell's rule. With reference to Fig. 12(b), the term $W(\lambda_1'',\lambda_3'',T)-W(\lambda_1',\lambda_3',T)$ represents the area under the stress-stretch curve between state λ_3' and state λ_3'', while the term $(\lambda_3''-\lambda_3')s^*$ represents the area the rectangle between the two states and under the horizontal line $s=s^*$. Consequently, (6.15) means that the value s^* should be chosen such that the two shaded areas in Fig. 12(b) are equal.

Fig. 14(a) plots a phase diagram on the (T,s) plane. As expected, the hydrogel is in the swollen phase when the temperature is low and the stress is high, and is in the shrunk phase when the temperature is high and the stress low. The two regions are separated by a curve, which is determined by calculating the stress using Maxwell's rule, e.g., (6.15), for every given temperature. Fig. 14 (b) and (c) plot the corresponding values λ_3' and λ_3'',λ_1' and λ_1'', respectively.

In the phase diagram on the (T,s) plane, each point on the curve separating the two regions corresponds to a state of coexistent phases. If T and s are prescribed, the proportion of the two phases is indeterminate. The situation is similar to a familiar phenomenon: a pure substance at the melting point can be a mixture of liquid and solid of any proportion. If the rod of the hydrogel is constrained to a fixed length l in the current state, however, the proportion of the two phases of can be determined. Solving (6.9) and (6.10) as simultaneous equations for L' and L'', we obtain the fraction of the shrunk phase

$$\frac{L'}{L}=\frac{\lambda_3''-l/L}{\lambda_3''-\lambda_3'}. \tag{6.16}$$

Recall that $l'=\lambda_3'L'$, and we can express the fraction in the current state.

$$\frac{l'}{l}=\left(\frac{L'}{L}\right)\left(\frac{L}{l}\right)\lambda_3'. \tag{6.17}$$

Fig. 14(d) plots the portion of the shrunk phase as a function of temperature when the total length of the rod is fixed as $l=2L$. At a low temperature, the swollen phase is predominant in the rod. The proportion of the shrunk phase increases with the temperature, and finally occupies the full length of the rod.

As the temperature varies, the shape of the surface $W(\lambda_1,\lambda_3,T)$ can change significantly; especially it may change from a non-convex shape to a globally convex shape beyond a particular temperature T_c. Beyond the critical temperature, only a single phase can exist. Based on the parameters used for the PNIPAM hydrogel, however, the free-energy surface $W(\lambda_1,\lambda_3,T)$ is non-convex for all temperatures. We have not found a critical temperature for such a system.

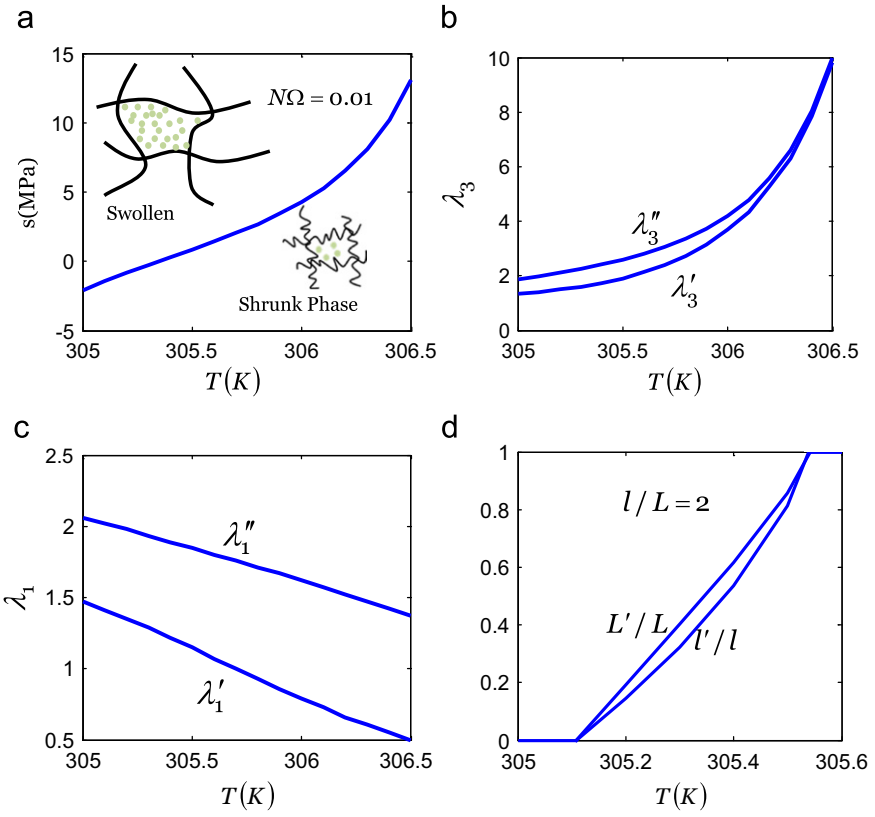

Fig. 14. (a) The phase diagram plotted on the temperature-stress plane for a rod subject to an axial stress and submerged in water. When two phases coexist in the rod in a state of equilibrium, various parameters in the two phases are functions of temperature: (b) The axial stretches in the two phases, (c) The transverse stretches in the two phases, and (d) The fraction of the shrunk phase as a function of the temperature.

7. Coexistent phases undergoing inhomogeneous deformation

Mechanical constraint often causes in the hydrogel a field of inhomogeneous deformation, and possibly a pattern of coexistent phases (e.g., Suzuki and Ishii, 1999; Bai and Suzuki, 1999). Deformation in each phase is often inhomogeneous. The phenomenon in general is complex, and requires numerical analysis. The governing equations, however, can be obtained readily by adapting the method of Eshelby (1956). Coexistent phases in hydrogels have been considered by Dolbow et al. (2004). Here we connect the general equations to the material model described in Sections 2 and 3. The results take a simple form, as summarized in words in the last paragraph of this section.

As illustrated in Fig. 15, a dry network is often taken to be the reference state. In the current state, the network equilibrates with a set of mechanical forces, and with an aqueous environment held at a fixed chemical potential of water μ and a fixed temperature T. In such a state of equilibrium, the chemical potential of water and the temperature in the hydrogel are homogeneous, and are equal to the values in the aqueous environment.

In equilibrium, the deformation in the hydrogel can be inhomogeneous. Name a small part of the network by the coordinate $\mathbf{X}$ of the part when the network is in the reference state. In the current state, the small part $\mathbf{X}$ moves to a place with coordinate x. The function $x(\mathbf{X})$ describes the deformation of the entire network. Define the deformation gradient F as

$$F_{iK} = \frac{\partial x_i(\mathbf{X})}{\partial X_K}. \tag{7.1}$$

The deformation gradient generalizes the notion of the stretches.

In equilibrium, the concentration of water in the hydrogel can also be inhomogeneous. Let $C(\mathbf{X})$ be the nominal concentration of water, namely, the number of water molecules in a small part of the hydrogel in the current state divided by the volume of the part in the reference state.

Let W be the nominal density of the Helmholtz free energy, namely, the Helmholtz free energy of a small part of the hydrogel in the current state divided by the volume of the part in the reference state. As a material model, the nominal density of the Helmholtz free energy is taken to be a function.

$$W = W(\mathbf{F}, C, T). \tag{7.2}$$

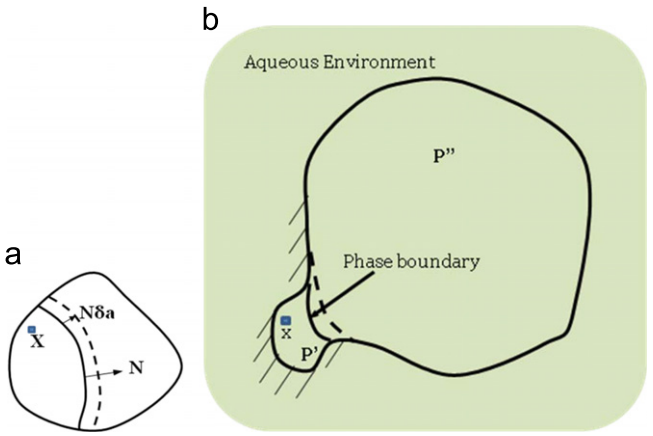

Fig. 15. Two phases, labeled as P' and P'', coexist in a hydrogel, and are separated by a phase boundary. (a) The referenced state is often taken to be the dry network subject to no forces. (b) In the current state, the network equilibrates with a solvent and a set of mechanical forces.

For convenience, introduce another quantity

$$\hat{W} = W - C\mu. \tag{7.3}$$

This quantity is a function of the deformation gradient, the chemical potential of water, and the temperature, namely

$$\hat{W} = \hat{W}(\mathbf{F},\mu,T). \tag{7.4}$$

The nominal stress s_{iK} is given by

$$s_{iK} = \partial \frac{\hat{W}(\mathbf{F},\mu,T)}{\partial F_{iK}}. \tag{7.5}$$

The true stress σ_{ij} relates to the nominal stress as

$$\sigma_{ij} = \frac{s_{iK}F_{jK}}{\det\mathbf{F}}. \tag{7.6}$$

Following Hong et al. (2008, 2009), we next describe a specific material model consistent with that in Sections 2 and 3. The volume of the hydrogel is taken to be the sum of the volume of the dry network and that of water in the hydrogel

$$\det\mathbf{F} = 1 + \Omega C. \tag{7.7}$$

This relation generalizes (2.5). Subject to the constraint (7.7), the concentration C is no long an independent variable, but is expressed in terms of the deformation gradient $\mathbf{F}$. Consequently, the Helmholtz free energy of the hydrogel takes the form $W(\mathbf{F},T)$. A combination of (7.4) and (7.7) gives that

$$\hat{W} = W(\mathbf{F},T) - \frac{(\det\mathbf{F}-1)\mu}{\Omega}. \tag{7.8}$$

Substituting (7.8) into (7.5) and (7.6), we obtain that

$$\sigma_{ij} = \frac{F_{jK}}{\det\mathbf{F}}\frac{\partial W(\mathbf{F},T)}{\partial F_{iK}} - \frac{\mu}{\Omega}\delta_{ij}. \tag{7.9}$$

This expression generalizes the equations of state written in terms of the principal stresses and principal stretches, (2.10)–(2.12). Within this formulation, a material model of the hydrogel is fully specified by the function $W(\mathbf{F},T)$. In particular, the Flory–Rehner model described in Section 3 can be written as such a function, with substitutions $\Omega C = \det\mathbf{F} - 1$, $\lambda_1\lambda_2\lambda_3 = \det\mathbf{F}$, and $\lambda_1^2 + \lambda_2^2 + \lambda_3^2 = F_{iK}F_{iK}$.

In the current state, the Helmholtz free energy of the hydrogel is $\int W dV$. The aqueous environment gives the hydrogel a total number $\int C dV$ of water molecules. Consequently, the aqueous environment lowers its Helmholtz free energy by $\mu\int C dV$. On each element of the volume of the hydrogel, $dV(\mathbf{X})$, we prescribe force $\mathbf{B}(\mathbf{X})dV$, where $\mathbf{B}$ is the nominal density of the body force. When the network is in the reference state, denote an element area of the surface of the hydrogel by $dA(\mathbf{X})$, and denote the unit vector normal to the element by $\mathbf{N}$, pointing outside the hydrogel. Parts of the surface of the hydrogel may be prescribed with displacement, and other parts of the surface of the hydrogel may be prescribed with forces. For example, on an element of the surface of the hydrogel, $dA(\mathbf{X})$, we may prescribe force $\mathbf{T}(\mathbf{X})dA$, where $\mathbf{T}$ is the nominal density of the surface force (i.e., the traction). The potential energy of the applied forces is $-\int B_i x_i dV - \int T_i x_i dA$.

The hydrogel, the aqueous environment, and the applied forces together constitute a thermodynamic system. The free energy of the system, Π, is the sum of the free energy of the hydrogel, the free energy of the aqueous environment, and the

potential energy of the applied forces

$$\Pi = \int W dV - \mu \int C dV - \int B_i x_i dV - \int T_i x_i dA \tag{7.10}$$

Thermodynamics requires that in equilibrium the free energy of the system be minimized as a functional of $x_i(\mathbf{X})$ and position of the phase boundary.

As illustrated in Fig. 15, in the hydrogel, two phases, labeled as P' and P'', may coexist. We track the boundary between the two phases in the reference state. When the network is in the reference state, denote the area of an element of the phase boundary by $dA(\mathbf{X})$, and denote the unit vector normal to the element by $\mathbf{N}$, pointing toward part P''. The displacement of hydrogel is continuous across the phase boundary

$$\mathbf{x}' = \mathbf{x}''. \tag{7.11}$$

We first keep the phase boundary fixed in the reference state, while vary the deformation of the hydrogel by $\delta x_i(\mathbf{X})$. Associated with this deformation, the free energy varies by

$$\delta\Pi = -\int \left(\frac{\partial s_{iK}}{\partial X_K} + B_i\right)\delta x_i dV + \int (s_{iK}N_K - T_i)\delta x_i dA + \int (s'_{iK} - s''_{iK})N_K \delta x_i dA. \tag{7.12}$$

The first integral is over the volume of the hydrogel. The second integral is over the surface of the hydrogel where traction is prescribed. The third integral is over the phase boundary. In equilibrium, $\delta\Pi = 0$ for arbitrary variation of the deformation $\delta x_i(\mathbf{X})$, so that (7.12) implies that

$$\frac{\partial s_{iK}}{\partial X_K} + B_i = 0, \tag{7.13}$$

in the volume of the hydrogel,

$$s_{iK}N_K = T_i, \tag{7.14}$$

on the surface of the hydrogel where traction is prescribe, and

$$(s'_{iK} - s''_{iK})N_K = 0, \tag{7.15}$$

on the phase boundary.

We next consider the variation of the free energy associated with the motion of the phase boundary. The motion of the phase boundary is tracked in the reference state. When the phase boundary moves by a distance $\delta\alpha(\mathbf{X})$, the element of the phase boundary moves from a part of the network, $\mathbf{X}$, to another part of the network, $\mathbf{X}+\mathbf{N}(\mathbf{X})\delta\alpha(\mathbf{X})$. Associated with the movement of the phase boundary, the free energy varies by (Eshelby, 1956; Abeyaratne and Knowles, 1990)

$$\delta\Pi = \int [(\hat{W}' - s'_{iK}F'_{iL}N_K N_L) - (\hat{W}'' - s''_{iK}F''_{iL}N_K N_L)]\delta\alpha dA. \tag{7.16}$$

The integral extends over the phase boundary. When the two phases are in equilibrium, $\delta\Pi = 0$ for arbitrary small movement of the phase boundary $\delta\alpha(\mathbf{X})$, so that the jump in front of $\delta\alpha(\mathbf{X})$ vanishes, giving

$$(\hat{W}' - s'_{iK}F'_{iL}N_K N_L) = (\hat{W}'' - s''_{iK}F''_{iL}N_K N_L). \tag{7.17}$$

This condition of equilibrium generalizes (6.15).

Thus, the coexistent phases satisfy usual governing equations of elasticity in each phase, and the continuity conditions (7.11), (7.15) and (7.17) across the phase boundary. The governing equations for a hydrogel in equilibrium with the aqueous environment and applied forces are identical to the governing equations for an elastic body in equilibrium with applied forces. So far as the conditions of equilibrium are concerned, the difference of a hydrogel from an elastic material is embodied in the choice of the free-energy function, $\hat{W}(\mathbf{F},\mu,T)$.

8. Concluding remarks

Following Flory and Rehner (1943), we assume that the free energy of mixing of polymers and water remains unchanged when the polymers are crosslinked into a network with a low crosslink density, and that the free energy of a hydrogel is the sum of the free energy of mixing and the free energy of stretching the network. We then use the free energy of mixing determined for the PNIPAM–water solutions to predict the behavior of the phase transition of the PNIPAM hydrogels under various mechanical forces and constraints. The predictions of the model agree well with experimental data for several cases of homogenous deformation in PNIPAM gels. The mechanical forces and constraints can greatly affect the amount of swelling, and can also change the phase-transition temperature. In extreme cases, the phase transition may be suppressed by mechanical constraint. We describe in some detail coexistent phases in a rod, and outline a theory of coexistent phases undergoing inhomogeneous deformation. It is hoped that the theory and examples described in this paper will stimulate further work in developing numerical methods and quantitative experiments.

Acknowledgements

This work is supported by the NSF for a project on Soft Active Materials (CMMI-0800161), and by the MRSEC at Harvard University.

References

Abeyaratne, R., Knowles, J.K., 1988. On the dissipative response due to discontinuous strains in bars of unstable elastic material. International Journal of Solids and Strucutres 24 (10), 1021–1044.
Abeyaratne, R., Knowles, J.K., 1990. On the driving traction acting on a surface of strain discontinuity in a continuum. Journal of the Mechanics and Physics of Solids 38 (3), 345–360.
Abeyaratne, R., Knowles, J.K., 1993. A continuum model of a thermoelastic solid capable of undergoing phase transitions. Journal of the Mechanics and Physics of Solids 41 (3), 541–571.
Afroze, F., Nies, E., Berghmans, H., 2000. Phase transitions in the system poly(*N*-isopropylacrylamide)/water and swelling behavior of the corresponding networks. Journal of Molecular Structure 554, 55–68.
An, Y.H., Solis, F.J., Jiang, H.Q., 2010. A thermodynamic model of physical gels. Journal of the Mechanics and Physics of Solids 58, 2083–2099.
Bai, G., Suzuki, A., 1999. Phase separation of weakly ionized polymer gels during shrinking phase transition. Journal of Chemical Physics 111 (22), 10338–10346.
Baek, S., Srinivasa, A.R., 2004. Diffusion of a fluid through an elastic solid undergoing large deformation. International Journal of Non-linear Mechanics 39, 201–218.
Baek, Pence, T.J., 2011. Inhomogeneous deformation of elastomer gels in equilibrium under saturated and unsaturated conditions. Journal of the Mechanics and Physics of Solids, 59, doi:10.1016/j.jmps.2010.12.013.
Bashir, R., Hilt, J.Z., Elibol, O., Gupta, A., Peppas, N.A., 2002. Micromechanical cantilever as an ultrasensitive pH microsensor. Applied Physics Letters 81, 3091–3093.
Berndt, I., Pedersen, J.S.F.J., Richtering, W., 2006a. Temperature-sensitive core–shell microgel particles with dense shell. Angewandte Chemie 118, 1769–1773.
Berndt, I., Popescu, C., Wortmann, F.J., Richtering, W., 2006b. Mechanics versus thermodynamics: swelling in multiple-temperature-sensitive core–shell microgels. Angewandte Chemie International Edition 45, 1081–1085.
Berndt, I., Richtering, W., 2003. Doubly temperature sensitive core–shell microgels. Macromolecules 36, 8780–8785.
Carpi, F., Smela, E. (Eds.), 2009. Biological Applications of Electroactive Polymer ActuatorsWiley.
Chester, S.A., Anand, L., 2010. A coupled theory of fluid permeation and large deformations for elastomeric materials. Journal of the Mechanics and Physics of Solids 58, 1879–1906.
Cho, E.C., Lee, J., Cho, K., 2003. Role of bound water and hydrophobic interactions in phase transition of poly(*N*-isopropylacrylamide) aqueous solution. Macromolecules 36, 9929–9934.
Doi, M., 2009. Gel dynamics. Journal of the Physical Society of Japan 78, 052001.
Dolbow, J., Fried, E., Jia, H.D., 2004. Chemically induced swelling of hydrogels. Journal of the Mechanics and Physics of Solids 52, 51–84.
Eichinger, B.E., Flory, P.J., 1968. Thermodynamics of polymer solutions. Part 1—natural rubber and benzene. Transactions of the Faraday Society 64, 2035–2053.
Eliassi, A., Modarress, H., Mansoori, G.A., 1999. Measurement of activity of water in aqueous poly(ethylene glycol) solutions (effect of excess volume on the Flory–Huggins-χ-parameter). Journal of Chemical and Engineering Data 44, 52–55.
Ericksen, J.L., 1975. Equilibrium of bars. Journal of Elasticity 5 (3-4), 191–201.
Eshelby, J.D., 1956. The continuum theory of lattice defects. Solid State Physics 3, 79–144.
Flory, P.J., 1942. Thermodynamics of high polymer solutions. Journal of Chemical Physics 10 (1), 51–61.
Flory, P.J., 1953. In: Principles of Polymer ChemistryCornell University Press, Ithaca, NY.
Flory, P.J., Rehner, J., 1943. Statistical mechanics of cross-linked polymer networks. II. Swelling. Journal of Chemical Physics 11 (11), 521–526.
Guenther, M., Gerlach, G., Corten, C., Kuckling, D., Muller, M., Shi, Z.M., Sorber, J., Arndt, K.F., 2007. Application of polyelectrolytic temperature-responsive hydrogels in chemical sensors. Macromolecular Symposia 254, 314–321.
Gibbs, J.W., 1873. A method of geometrical representation of the thermodynamic properties of substances by means of surfaces. Transactions of the Connecticut Academy 2, 382–404 (Available online at Google Books).
Harmon, M.E., Kuckling, D., Pareek, P., Frank, C.W., 2003. Photo-cross-linable PNIPAAm copolymers. 4. Effects of copolymerization and cross-linking on the volume-phase transition in constrained hydrogel layers. Langmuir 19, 10947–10956.
Hong, W., Zhao, X.H., Zhou, J.X., Suo, Z.G., 2008. A theory of coupled diffusion and large deformation in polymeric gels. Journal of the Mechanics and Physics of Solids 56, 1779–1793.
Hong, W., Liu, Z.S., Suo, Z.G., 2009. Inhomogeneous swelling of a gel in equilibrium with a solvent and mechanical load. International Journal of Solids and Structures 46, 3282–3289.
Hong, W., Zhao, X.H., Suo, Z.G., 2010. Large deformation and electrochemistry of polyelectrolyte gels. Journal of the Mechanics and Physics of Solids 5, 558–577.
Hirotsu, S., Onuki, A., 1989. Volume phase transition of gels under uniaxial tension. Journal of The physical Society of Japan 58 (5), 1508–1511.
Hu, Z.B., Zhang, X.M., Li., Y., 1995. Synthesis and application of modulated polymer gels. Science 260, 525–527.
Huggins, M.L., 1941. Solutions of long chain compounds. Journal of Chemical Physics 9 (5), 440.
Huggins, M.L., 1964. A revised theory of high polymer solutions. Journal of Chemical Physics 86 (17), 3535–3540.
Hui, C.Y., Muralidharan, V., 2005. Gel mechanics: a comparison of the theories of Biot and Tanaka, Hocker, and Benedek. The Journal of Chemical Physics 123, 154905.
Juodkazis, S., Mukai, N., Wakaki, R., Yamaguchi, A., Matsuo, S., Misawa, H., 2000. Reversible phase transitions in polymer gels induced by radiation forces. Nature 408, 178–181.
Lee, Y.J., Braun, P.V., 2003. Tunable inverse opal hydrogel pH sensors. Advanced Materials 15 (7-8), 563–566.
Li, H., Luo, R., Birgersson, E., Lam, K.Y., 2007. Modeling of multiphase smart hydrogels responding to pH and electric voltage coupled stimuli. Journal of Applied Physics 101, 114905.
Linden, H.V., Olthuis, W., Bergveld, P., 2004. An efficient method for the fabrication of temperature-sensitive hydrogel microactuators. Lab on a Chip 4, 619–624.
Marcombe, R., Cai, S.Q., Hong, W., Zhao, X.H., Lapusta, Y., Suo, Z.G., 2010. A theory of constrained swelling of a pH-sensitive hydrogel. Soft Matter 6, 784–793.
Masuda, F., 1994. Trends in the development of superabsorbent polymers for diapers, pp. 88-89. In: Superabsorbent Polymers. ACS Symposium Series, vol. 573.
Oh, K.S., Oh, J.S., Choi, H.S., Bae, Y.C., 1998. Effect of cross-linking density on swelling behavior of NIPA gel particles. Macromolecules 31, 7328–7335.
Osada, Y., Gong, J.P., 1998. Soft and wet materials: polymer gels. Advanced Materials 10 (11), 827–837.
Otake, K., Inomata, H., Konno, M., Saito, S., 1990. Thermal analysis of the volume phase transition with *N*-isopropylacrylamide gels. Macromolecules 23 (1), 283–289.

Richter, A., Howitz, S., Kuckling, D., Amdt., K.F., 2004. Influence of volume phase transition phenomena on the behavior of hydrogel-based vavles. Sensors and Actuators B 99, 451–458.
Sastry, N.V., Patel, M.C., 2003. Densities, excess molar volumes, viscosities, speeds of sound, excess isentropic compressibilities, and relative permittivities for alkyl (methyl, ethyl, butyl, and isoamyl) acetates+glycols at different temperatures. Journal of Chemical and Engineering Data 48, 1019–1027.
Schild, H.G., 1992. Poly (*N*-isopropylacrylamide): experiment, theory and application. Progress in Polymer Science 17, 163–249.
Shibayama, M., Shirotani, Y., Hirose, H., Nomura, S., 1997. Simple scaling rules on swollen and shrunken polymer gels. Macromolecules 30 (23), 7307–7312.
Shiga, T., 1997. Deformation and viscoelastic behavior of polymer gels in electric fields. Advances in Polymer Science 134, 131–163.
Steinberg, I.Z., Oplatka, A., Katchalsky, A., 1966. Mechanochemical engines. Nature 210, 568–571.
Suzuki, A., Ishii, T., 1999. Phase coexistence of neutral polymer gels under mechanical constraint. Journal of Chemical Physics 110 (4), 2289–2296.
Suzuki, A., Yoshikawa, S., Bai, G., 1999. Shrinking pattern and phase transition velocity of poly(*N*-isopropylacrylmide) gel. Journal of Chemical Physics 111 (1), 360–367.
Suzuki, A., Sanda, K., Omori, Y., 1997. Phase transition in strongly stretched polymer gels. Journal of Chemical Physics 107 (13), 5179–5185.
Tanaka, T., Fillmore, D., Sun, S.T., Nishio, I., Swislow, G., Shah, A., 1980. Phase transition in ionic gels. Physical Review Letters 45 (20), 1636–1639.
Vidyasagar, A., Majewski, J., Toomey, R., 2008. Temperature induced volume-phase transition in surface-tethered poly(*N*-isopropylacrylamide) networks. Macromoleclues 41, 919–924.
Yoon, J.W., Cai, S.Q., Suo, Z.G., Hayward, R.H., 2010. Poroelastic swelling kinetics of thin hydrogel layers: comparison of theory and experiment. Soft Matter 6, 6004–6012.